BIOCHEMISTRY
including biophysical chemistry & molecular biology
Article

Biochemistry **2010,** *49,* 1737–1743 1737
DOI: 10.1021/bi901323a

A Structural Model for the Single-Stranded DNA Genome of Filamentous Bacteriophage Pf1[†]

Masamichi Tsuboi,[‡] Masaru Tsunoda,[‡] Stacy A. Overman,[§] James M. Benevides,[§] and George J. Thomas, Jr.*[,§]

[‡]*College of Science and Engineering and Faculty of Pharmacy, Iwaki-Meisei University, Chuodai-Iino 5-5-1, Iwaki, Fukushima 970-8551, Japan, and* [§]*School of Biological Sciences, University of Missouri-Kansas City, 5100 Rockhill Road, Kansas City, Missouri 64110-2499*

Received July 30, 2009; Revised Manuscript Received January 14, 2010

ABSTRACT: The filamentous bacteriophage Pf1, which infects strain PAK of *Pseudomonas aeruginosa*, is a flexible filament (∼2000 × 6.5 nm) consisting of a covalently closed DNA loop of 7349 nucleotides sheathed by 7350 copies of a 46-residue α-helical subunit. The subunit α-helices, which are inclined at a small average angle (∼16°) from the virion axis, are arranged compactly around the DNA core. Orientations of the Pf1 DNA nucleotides with respect to the filament axis are not known. In this work we report and interpret the polarized Raman spectra of oriented Pf1 filaments. We demonstrate that the polarizations of DNA Raman band intensities establish that the nucleotide bases of packaged Pf1 DNA are well ordered within the virion and that the base planes are positioned close to parallel to the filament axis. The present results are combined with a previously proposed projection of the intraviral path of Pf1 DNA [Liu, D. J., and Day, L. A. (1994) *Science 265*, 671−674] to develop a novel molecular model for the Pf1 assembly.

The filamentous bacterial viruses (*Inovirus*) are members of a genus of morphologically similar virions that infect different bacteria via molecular recognition of a host-specific pilin (*2*). Each packages a single-stranded (ss)[1] DNA genome within a long and thin flexible capsid of either class I (5-start helix, C_2S_5) or class II (1-start helix, $C_1S_{5.4}$) symmetry (*3*). The class II Pf1 virion (∼2000 × ∼6.5 nm), which infects *Pseudomonas aeruginosa* strain PAK, is about twice the length of other well-characterized filamentous bacteriophages and is the most easily drawn into highly ordered fibers that are amenable to X-ray diffraction (*4*), solid-state NMR (*5*), and polarized spectroscopic (*6*) analyses. Liquid crystalline arrays of Pf1 are also effective for the alignment of associated macromolecules, a phenomenon that facilitates the measurement of dipolar couplings in NMR structure determinations (*7*, *8*). Like other filamentous bacteriophages, Pf1 provides an attractive model for studying molecular mechanisms of nucleoprotein assembly and membrane transport.

The Pf1 virion comprises a ssDNA loop of 7349 nucleotides sheathed by 7350 copies of a 46-residue α-helical subunit ([1]GVIDTSAVES [11]AITDGQGDMK [21]AIGGYIVGAL [31]VILAVAGLIY [41]SMLRKA) plus a few copies of minor proteins at the filament ends. The capsid subunits of Pf1 provide the only known example of filamentous bacteriophage architecture exhibiting a nucleotide-to-subunit ratio of 1:1 (*3*). Although Pf1 structure has been investigated by a variety of methods over the past few decades (*1*, *4*−*6*, *9*−*21*), relatively little is known about the overall organization of the ssDNA genome within the capsid and the specific orientations of DNA nucleotides with respect to the filament axis. A loop of ssDNA at the capsid core and spanning its length is feasible if the deoxyribosyl−phosphate backbones of the two apposing antiparallel strands are proximal to the virion axis and the bases project distally from the axis (*1*, *16*, *22*). In this model, termed *P*-DNA (*1*), the proposed nucleotide axial repeat of 6 Å is about 75% greater than that of canonical *B*-DNA. Raman and ultraviolet−resonance Raman (UVRR) studies of Pf1 have established that the packaged Pf1 DNA molecule incorporates C2′-*endo*/*anti* deoxyribosyl sugar puckers as well as unpaired and unstacked bases, structural features that are consistent with a *P*-DNA-like conformation (*6*, *17*, *20*, *23*, *24*). Such an axially extended *P*-DNA structure exhibiting phosphates "in" and bases "out" has also been suggested as a prototype for DNA molecules subjected to high mechanical or torsional stress (*25*−*27*).

In previous work we have implemented methods of polarized Raman spectroscopy (*28*) in conjunction with known Raman tensors (*29*) to determine the axial orientations of several molecular subgroups of the ssDNA genome and capsid subunits in oriented fibers of the native Pf1 virus (*6*, *19*). Here, we further exploit this methodology to revise the structural model of Pf1 proposed by Liu and Day on the basis of X-ray fiber diffraction studies (*1*). Because our goal is to refine the Liu and Day model by determining additional structural details of the packaged Pf1 DNA molecule, including the orientations of the nucleotide purine and pyrimidine rings with respect to the viral filament axis, we have not evaluated alternative DNA structural models that might also be consistent with the polarized Raman data. We use these new results in combination with previously determined structural constraints to propose a novel model for the native Pf1 assembly.

EXPERIMENTAL PROCEDURES

Sample Preparation. Wild-type Pf1 virus was grown using *P. aeruginosa* strain PAK as the host in MS medium containing 1% glucose and 4 mM $CaCl_2$. Mature viral particles, extruded through the bacterial cell membrane and into the growth medium, were collected by precipitation with poly(ethylene glycol) (2%) and NaCl (0.5 M) followed by low-speed centrifugation. The virus precipitate was resuspended in 10 mM Tris (pH 7.8 ± 0.2), and the resulting suspension was purified by four

[†]Supported by NIH Grants GM50776 and GM54378.
*Author to whom correspondence should be addressed: telephone, 816-235-5247; telefax, 816-235-1503; e-mail, thomasgj@umkc.edu.
[1]Abbreviations: Pf1, a class II filamentous virus; ss, single stranded; NMR, nuclear magnetic resonance; UVRR, ultraviolet−resonance Raman.

Published on Web 01/15/2010

cycles of pelleting at 330000*g* for 1.5 h and resuspension of the pellet in 10 mM Tris buffer. This procedure accomplishes essentially complete removal of excess NaCl (*20*). Typically, 30−50 mg of purified Pf1 is obtained per liter of growth medium. Pf1 concentration was determined by UV spectrophotometry assuming a molar extinction coefficient ε_{270} = 2.06 mL·mg^{-1}·cm^{-1} (*30*). Growth media and reagents were obtained from Sigma-Aldrich (St. Louis, MO) and Fisher Scientific (Pittsburgh, PA).

Oriented Pf1 fibers of ~0.5 mm thickness were prepared for polarized Raman spectroscopy by slowly drawing a droplet of Pf1 solution (~100 mg/mL in 10 mM Tris, pH 7.8) in a fiber pulling device maintained at 20 °C and 92% relative humidity (*6*). The oriented fiber was sealed in a hygrostatic chamber and placed on the microscope stage for subsequent polarized Raman measurements. Samples contained >95% of Pf1 particles oriented unidirectionally (*31*).

Raman Instrumentation. Polarized Raman spectra were excited at 532 nm using a Nd:YVO_4 laser (model Millenium-V; Spectra Physics Inc., Mountain View, CA) and collected on a microspectrophotometer (model Labram Infinity; Jobin-Yvon Inc., Edison, NJ) equipped with a polarizing microscope (model BX-40; Olympus America Inc., Melville, NY). The radiant power at the laser head was maintained at 200 mW. The laser beam was directed into the 40× objective of the microscope and onto the oriented fiber of the filamentous bacteriophage through a cover glass that sealed the specimen within a hygrostatic chamber maintained at 92% relative humidity. The backscattered (180°) Raman photons were collected with the same objective and then passed through a notch filter, polarization analyzer, and scrambler to the entrance slit of the Labram Infinity polychromator. Raman scattered photons were detected using a low-temperature, charge-coupled device detector (model Spectrum One; SPEX Inc., Edison, NJ).

Polarized Raman spectra were also excited at 632.8 nm using the dedicated He−Ne laser of the Labram Infinity. The data were collected and analyzed as noted above. The radiant power at the He−Ne laser head did not exceed 100 mW.

We note that the above system provides superior throughput and resolution for polarization studies compared to an earlier Raman microprobe analysis that utilized a beam splitter and triple monochromator (*6*). In effect, weak spectral features are better resolved and may appear more pronounced than in a previous polarized Raman study of Pf1 (*6*).

Raman Spectral Polarization. The polarized Raman spectra are characterized by the measured spectral intensities (I_{ij}) for specified polarization axes of the incident (i = b, c) and scattered (j = b, c) radiation with respect to the axis (c) of orientation of the Pf1 fiber. The polarized Raman spectra I_{cc} and I_{cb} were measured respectively by maintaining the fiber in a fixed orientation and then rotating the polarization analyzer by 90°. These intensities correspond to the fiber tensor components cc and cb, respectively, where *c* is the fiber (virion) axis and *b* is perpendicular to *c*. Rotation of the fiber by 90° on the microscope platform allows I_{bb} and I_{bc} to be measured in succession using the same procedure as above. If the laser beam is precisely focused on the same portion of the sample throughout this protocol, then we expect $I_{cb} = I_{bc}$. This was the case in the present experiments. Further details regarding the measurement of polarized Raman spectra of oriented fibers of filamentous viruses and the quantitative analyses of the spectral data have been described (*28*, *29*). Here, we report the polarized Raman spectra (I_{cc}, I_{bb}, I_{bc}, I_{cb}) used in subsequent calculations.

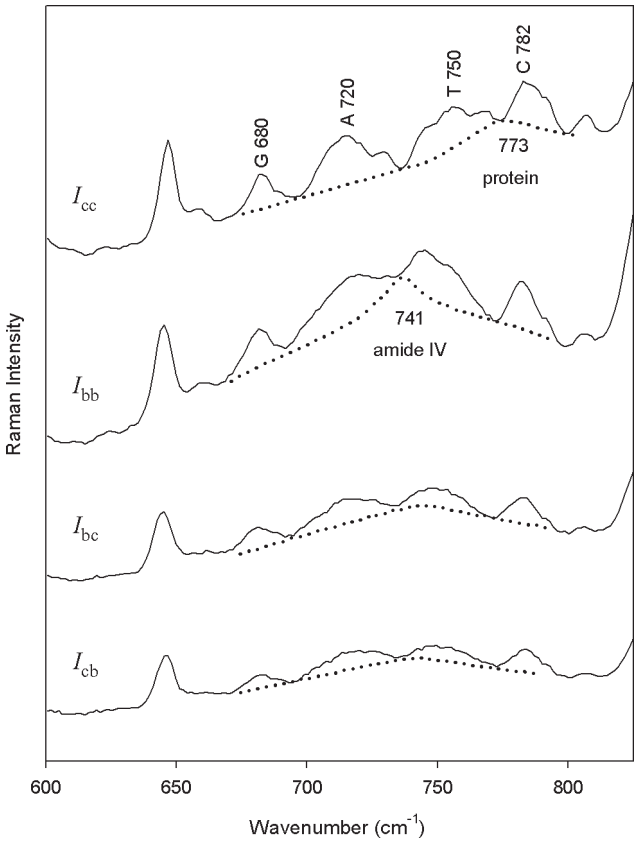

FIGURE 1: Polarized Raman spectral intensities (I_{cc}, I_{bb}, I_{bc}, and I_{cb}) obtained from an oriented fiber of Pf1 using 532 nm excitation. Contributions from Pf1 DNA nucleotides in the interval 600−850 cm^{-1} are labeled. Raman bands assigned to coat protein tyrosines (640 cm^{-1}) and other protein residues (dashed lines) are also indicated (*6*, *36*).

RESULTS AND INTERPRETATION

Raman Spectral Data. Polarized Raman spectra (I_{cc}, I_{bb}, I_{bc}, I_{cb}) representative of oriented Pf1 fibers are shown in Figures 1 and 2 for excitation wavelengths of 532 and 632.8 nm, respectively. Similar spectral data at both excitation wavelengths were collected from at least five independently prepared Pf1 fibers. Here, we are concerned with the Raman bands that are diagnostic of the four DNA bases of packaged Pf1 DNA and for which Raman tensors are available, namely, those assigned to the purine and pyrimidine ring breathing modes at 680 (guanine), 720 (adenine), 750 (thymine), and 782 (cytosine) cm^{-1} (*9*, *12*). Table 1 shows the polarized Raman intensity ratios I_{cc}/I_{bb} and I_{cc}/I_{bc} obtained and averaged from the five sets of Pf1 spectra. The results demonstrate that within the estimated limits of experimental error the polarized Raman intensity ratios are independent of excitation wavelength. We note that the relatively large error estimate in I_{cc}/I_{bb} for the 750 cm^{-1} band of thymine is due primarily to overlap of the thymine marker with an underlying broad band near 741 cm^{-1}, which is attributable to the α-helix amide IV mode of the capsid subunit.

DNA Base Orientations. For each of the Raman markers of the packaged Pf1 DNA molecule (Table 1), we find that $I_{cc}/I_{bb} > 1$, which indicates that each type of base residue is on average nonrandomly oriented with respect to the viral filament axis (*c*) (*29*). To determine the average base orientations from the observed I_{cc}/I_{bb} values of specific Raman markers (680, 720, 750, and 782 cm^{-1} bands), we require the corresponding Raman tensors. These tensors, which have been determined from studies of oriented fibers of

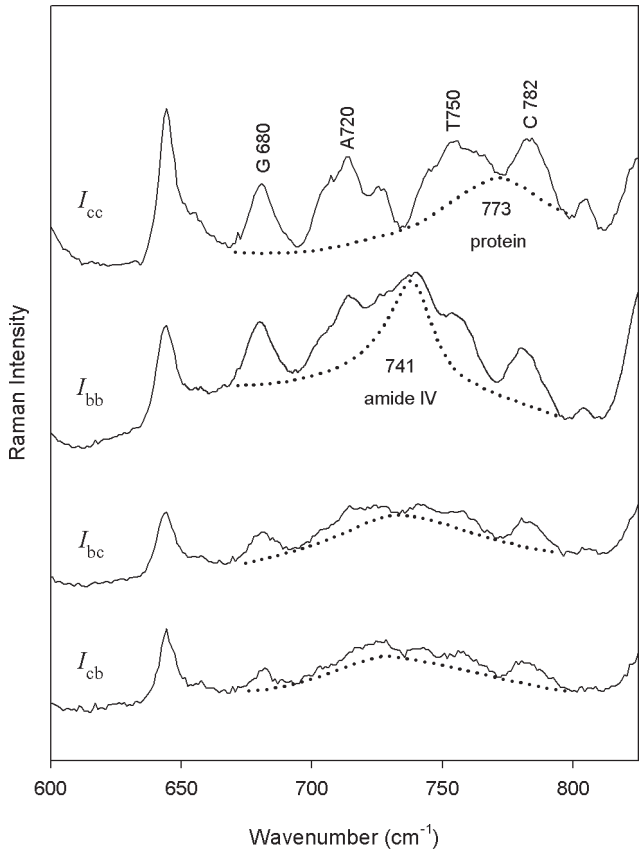

FIGURE 2: Polarized Raman spectral intensities (I_{cc}, I_{bb}, I_{bc}, and I_{cb}) obtained from an oriented fiber of Pf1 using 632.8 nm excitation. Contributions from nucleotides in the interval 600−850 cm^{-1} are labeled. Raman bands of coat protein tyrosines (640 cm^{-1}) and other residues (dashed line) are also indicated (*6*, *36*).

double-helical *B*-DNA (*32*), are assumed to be transferable to the nucleosides of Pf1 DNA because the latter incorporate the same canonical C2′-*endo*/*anti* nucleoside conformations. The tensors (defined by $r_1 = \alpha_{xx}/\alpha_{zz}$ and $r_2 = \alpha_{yy}/\alpha_{zz}$) are given in Figure 3. In each case, the tensor principal axis z is perpendicular to the base plane, while both x and y are in the base plane, as shown.

The orientation of a given DNA base residue (i = A, C, G, T) in the oriented Pf1 fiber can be represented by specifying the two Eulerian angles, θ_i and χ_i, where θ_i is the angle between the fiber axis (c) and the normal (z) to the plane of base i and χ_i is the angle between the y axis and the line (O−N) that represents the intersection between the xy plane of base i and the fiber ab plane (perpendicular to c or z) (*29*). For each base i the polarized Raman intensity ratios $[I_{cc}/I_{bb}]_i$ and $[I_{cc}/I_{bc}]_i$ are related to θ_i, χ_i, r_{1i}, and r_{2i} by eqs 1 and 2.

$$[I_{cc}/I_{bb}]_i = 4[r_{1i}\sin^2\theta_i\cos^2\chi_i + r_{2i}\sin^2\theta_i\sin^2\chi_i + \cos^2\theta_i]^2/ [r_{1i}(\cos^2\theta_i\cos^2\chi_i + \sin^2\chi_i) + r_{2i}(\cos^2\theta_i\sin^2\chi_i + \cos^2\chi_i) + \sin^2\theta_i]^2 \quad (1)$$

$$[I_{cc}/I_{bc}]_i = 2[r_{1i}\sin^2\theta_i\cos^2\chi_i + r_{2i}\sin^2\theta_i\sin^2\chi_i + \cos^2\theta_i]^2/ [\sin^2\theta_i\cos^2\theta_i(r_{1i}\cos^2\chi_i + r_{2i}\sin^2\chi_i - 1)^2 + (\sin^2\theta_i\sin^2\chi_i\cos^2\chi_i)(r_{1i} - r_{2i})^2] \quad (2)$$

(*A*) *Guanine*. Use of eq 1 with the guanine Raman tensors ($r_{1G} = 0.2$, $r_{2G} = 3.3$) and the polarized Raman intensity ratio for the guanine 680 cm^{-1} marker ($[I_{cc}/I_{bb}]_G = 1.26 \pm 0.05$) at the lower (1.21) and upper (1.31) experimental limits yields the two contours drawn in θ_G,χ_G space as solid lines in Figure 4a. Similarly, with corresponding $[I_{cc}/I_{bc}]_G$ data eq 2 yields the two contours represented as dashed lines in Figure 4a. The range of θ_G,χ_G values allowed for the orientation of the average guanine ring is given by the area enclosed within the four contour lines, whence $\theta_G = 63 \pm 2°$ and $\chi_G = 45.5 \pm 1.0°$.

(*B*) *Adenine*. Corresponding application of eqs 1 and 2 with $[I_{cc}/I_{bb}]_A = 1.30 \pm 0.10$, $I_{cc}/I_{bc} = 3.9 \pm 0.2$ for the adenine 720 cm^{-1} band ($r_{1A} = 0.35$, $r_{2A} = 2.6$) yields the results shown in Figure 4b. Accordingly, for adenine $\theta_A = 63 \pm 4°$ and $\chi_A = 47 \pm 2°$.

(*C*) *Thymine*. Similarly, the θ_T,χ_T plot generated for thymine by eqs 1 and 2 and the data for the 750 cm^{-1} band ($[I_{cc}/I_{bb}]_T = 1.30 \pm 0.20$, $[I_{cc}/I_{bc}]_T = 3.3 \pm 0.2$, $r_{1T} = 2.2$, $r_{2T} = 0.2$) is shown in Figure 4c, which gives $\theta_T = 68 \pm 8°$ and $\chi_T = 45 \pm 2°$.

(*D*) *Cytosine*. Finally, application of eqs 1 and 2 for the cytosine 782 cm^{-1} band ($[I_{cc}/I_{bb}]_C = 1.24 \pm 0.05$, $[I_{cc}/I_{bc}]_C = 2.6 \pm 0.1$, $r_{1C} = 2.6$, $r_{2C} = 0.1$) yields $\theta_C = 67 \pm 3°$ and $\chi_C = 44 \pm 2°$ (Figure 4d).

Pf1 DNA Atomic Coordinates. Coordinates proposed previously for the backbone of packaged Pf1 DNA (*1*) and geometric data specific to base residues A, C, G, and T (*33*) were combined with presently determined base orientation angles (θ_i,χ_i values) to calculate refined atomic coordinates for each Pf1 nucleotide base. (Here, we reference the coordinates deposited previously by Liu and Day in the Protein Data Bank by the notation AMP0LD.pdb, CMP0LD.pdb, GMP0LD.pdb, and TMP0LD.pdb (*1*).) To illustrate our approach, we consider the case of cytosine. With the Raman tensor of the 782 cm^{-1} cytosine marker defined such that the tensor y axis is parallel to the line intersecting ring atoms C2 and C4, the tensor x axis is perpendicular to y in the base plane, and the tensor z axis is normal to the base plane (Table 1 and Figure 3), we obtain $\theta_C = 63°$ and

Table 1: Coordinates of Pf1 DNA Bases

	guanine	adenine	thymine	cytosine
Experimental Data				
Raman (cm^{-1})	680	720	750	782
I_{cc}/I_{bb}	1.26 ± 0.05	1.30 ± 0.10	1.30 ± 0.20	1.24 ± 0.05
I_{cc}/I_{bc}	2.6 ± 0.1	3.9 ± 0.2	3.3 ± 0.2	2.6 ± 0.1
tensor axes	G2	G2	C3	C3
r_1	0.20	0.35	2.2	2.6
r_2	3.3	2.6	0.20	0.10
θ^a (deg)	63 ± 2 (63)	63 ± 4 (63)	68 ± 8 (63)	67 ± 3 (63)
χ^a (deg)	45 ± 1 (26)	47 ± 2 (17)	45 ± 2 (44)	44 ± 2 (47)
rotation angle (deg)	16	19	5	4
rotation axis	⊥ plane at C1*	⊥ plane at C1*	C1*−N1	C1*−N1
PDB reference[b]	GMP0LD	AMP0LD	TMP0LD	CMP0LD
Proposed Coordinates				
θ,χ (deg)	63, 46	63, 47	68, 44	67, 46
PDB reference[c]	GMP0MT	AMP0MT	TMP0MT	CMP0MT
rotation (deg)	35.5	263.7	131.8	0
rise (Å)	18.3	12.2	6.1	0
up strand	GMP6MT	AMP4MT	TMP2MT	CMP0MT
down strand	GMP7MT	AMP5MT	TMP3MT	CMP1MT

[a]Values in parentheses are based upon energy minimization of the proposed structure of Liu and Day (*1*). See text. [b]Data of Liu and Day (*1*). [c]Coordinates are available from the authors upon request.

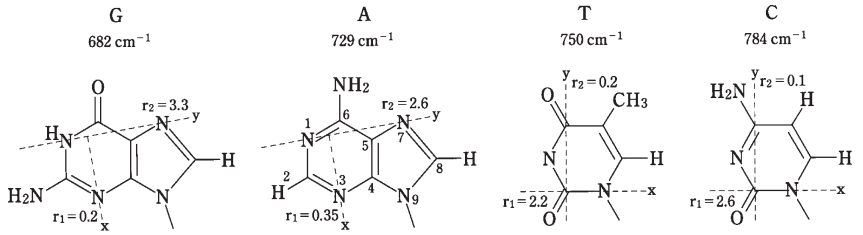

FIGURE 3: Raman tensors associated with the vibrational modes of the Pf1 DNA bases that are labeled in Figures 1 and 2. The in-plane tensor principal axes (*x* and *y*) are indicated by broken lines; principal axis *z* is perpendicular to the *xy* plane. The Raman tensor ratios, $r_1 = \alpha_{xx}/\alpha_{zz}$ and $r_2 = \alpha_{yy}/\alpha_{zz}$, are also indicated.

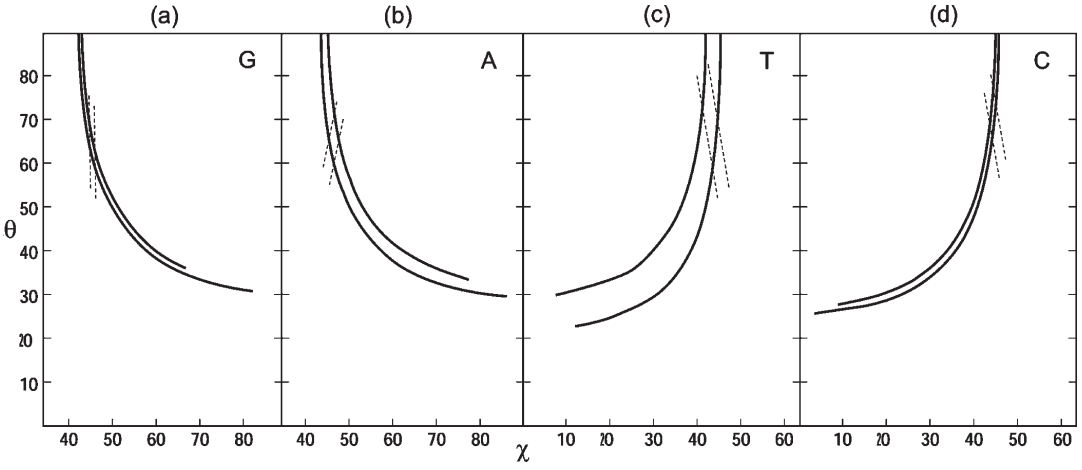

FIGURE 4: Contour maps in θ,χ space showing the I_{cc}/I_{bb} and I_{cc}/I_{bc} values for the Pf1 DNA Raman markers of Figures 1 and 2. (a) Raman marker of G (682 cm^{-1}). Solid lines show contours corresponding to limiting I_{cc}/I_{bb} values (1.21 and 1.31). Broken lines show contours corresponding to limiting I_{cc}/I_{bc} values (2.5 and 2.7). The parallelogram represented by the area between solid and broken lines defines the allowed ranges of θ and χ, i.e., $I_{cc}/I_{bb} = 1.26 \pm 0.05$ and $I_{cc}/I_{bc} = 2.6 \pm 0.1$, which restrict the θ,χ pair to $63 \pm 2°$, $45.5 \pm 1.0°$. (b) Corresponding data for the Raman marker of A (720 cm^{-1}). $I_{cc}/I_{bb} = 1.30 \pm 0.10$ and $I_{cc}/I_{bc} = 3.9 \pm 0.2$, which restrict the θ,χ pair to $63 \pm 4°$, $47 \pm 2°$. (c) Corresponding data for the Raman marker of T (750 cm^{-1}). $I_{cc}/I_{bb} = 1.30 \pm 0.20$ and $I_{cc}/I_{bc} = 3.3 \pm 0.2$, which restrict the θ,χ pair to $68 \pm 8°$, $45 \pm 2°$. (d) Corresponding data for the Raman marker of C (784 cm^{-1}). $I_{cc}/I_{bb} = 1.24 \pm 0.05$ and $I_{cc}/I_{bc} = 2.6 \pm 0.1$, which restrict the θ,χ pair to $67 \pm 3°$, $44 \pm 2°$.

$\chi_C = 47°$. Experimentally, however, we observed that $\theta_C = 67°$ (Figure 4d). Accordingly, the cytosine base requires a rotation of 4° about the C1*−N1 bond to generate a refined set of coordinates (labeled CMP0MT) that is consistent with the experimental results. The CMP0LD and CMP0MT structures are compared in Figure 5.

We applied the same procedure to refine the existing PDB coordinates (*1*) of the A, G, and T nucleotides to achieve consistency with the corresponding experimental results. The required rotations about the nucleoside glycosyl bonds are 19° for χ_A, 16° for χ_G, and 5° for χ_T. The refined coordinates for AMP0MT, GMP0MT, and TMP0MT lead to the entries of Table 1. The AMP0MT structure is shown in the top of Figure 6.

The structures AMP0MT, CMP0MT, GMP0MT, and TMP0MT correspond to one strand ("up" strand) of the packaged ssDNA loop. The coordinates of the apposing ("down") strand, which are designated as AMP1MT, CMP1MT, GMP1MT, and TMP1MT, respectively, are generated by an operation comprising a 180° dyad rotation, a 6.10 Å translation along *c*, and a −114° rotation about *c* (matrix 1 (*1*)). The CMP1MT and AMP1MT structures are shown in Figures 5 (bottom) and 6 (middle), respectively. Extension of the DNA up and down strands within the context of the Pf1 capsid assembly involves successive operations of rotation by 131.84° about *c* in combination with a 6.10 Å translation along *c*. An example of an extended DNA segment, consisting of eight nucleotides (up strand, CMP0MT, TMP2MT, AMP4MT, GMP6MT; down strand, CMP1MT, TMP3MT, AMP5MT, GMP7MT), is depicted in Figure 7. In the discussions which follow we refer to this DNA structure as *Pf1*-DNA.

Finally, we include in the *Pf1*-DNA model of Figure 8 a set of eight subunits (SubI, where I = 0, ..., 7) of the Pf1 capsid, the coordinates of which were obtained from the 1PFI model of Marvin and co-workers (*34*). The capsid subunits are related to one another by the operations of a rotation by 65.92° about *c* and a translation of 3.05 Å along *c*, consistent with the operations that interrelate the nucleotides of encapsidated Pf1 DNA (*1*).

Model for the Pf1 Virion. The procedure above generates coordinates for a segment of the Pf1 virion comprising 8 of the 7350 nucleotides of encapsidated Pf1 DNA and an equivalent number of capsid subunits. The coordinates (labeled Pf1N8P8*) of this segment include nucleotides numbered as CMP0MT = 801, TMP2MT = 802, AMP4MT = 803, GMP6MT = 804, GMP7MT = 805, AMP5MT = 806, TMP3MT = 807, and CMP1MT = 808 and subunits numbered as Sub0 = 1 (or 46), Sub1 = 101 (146), Sub2 = 201 (246), Sub3 = 301 (346), Sub4 = 401 (446), Sub5 = 501 (546), Sub6 = 601 (646), and Sub7 = 701 (746). In this coordinate set we found five steric clashes, two of which involved subunit/subunit interferences (Val31 Cγ1···Leu343 Cδ1, Val431 Cγ1···Leu743 Cδ1) and three of which involved subunit/nucleotide interferences (C801 O2···Arg144 Cζ, T802 C7···Lys545 Cγ, Ade803 N3···Arg344 Nη). Clashes were eliminated by use of the CNS program (*35*). Energy minimization was carried out by allowing fluctuations in the coordinates of side chain atoms (Cβ and beyond) of the amino acids Val31, Arg144, Arg244, Leu343, Arg344,

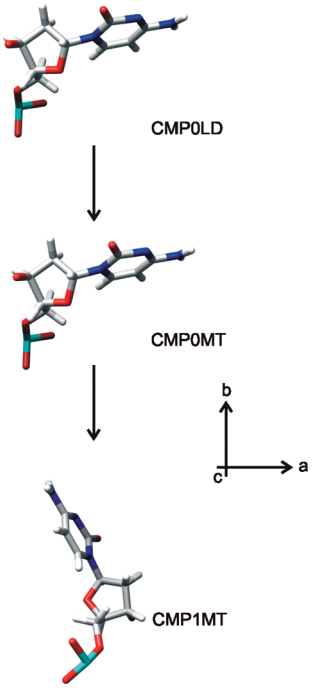

FIGURE 5: Structures of cytidylic acid residues of Pf1 DNA as modeled by Liu and Day (CMP0LD (*1*)) and in the present analysis (CMP0MT and CMP1MT; see text). The views are along the direction of the virion axis (*c*). Note that CMP0MT is derived from coordinates of CMP0LD by rotating the cytosine moiety by 4° around the C1*−N1 bond to achieve consistency with the experimental θ,χ values (67°, 44°); CMP1MT represents a residue of the apposing strand and is derived from CMP0MT by applying the appropriate rotation/translation matrix (*1*).

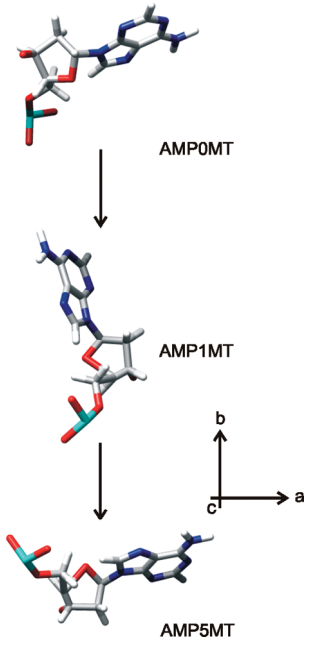

FIGURE 6: Structures of adenylic acid residues of Pf1 DNA viewed along the direction of the virion axis (*c*). AMP0MT is derived from the coordinates of AMP0LD (*1*) and data of Saenger (*33*) followed by a rotation of the adenine moiety by 19° about an axis perpendicular to its plane to achieve consistency with the experimental value of χ (47°). AMP1MT represents a residue of the apposing strand and is derived from AMP0MT by applying the appropriate rotation/translation matrix (*1*). AMP5MT is derived from AMP1MT by a further rotation of 263.7° about the virion axis and translation of 12.2 Å along the axis.

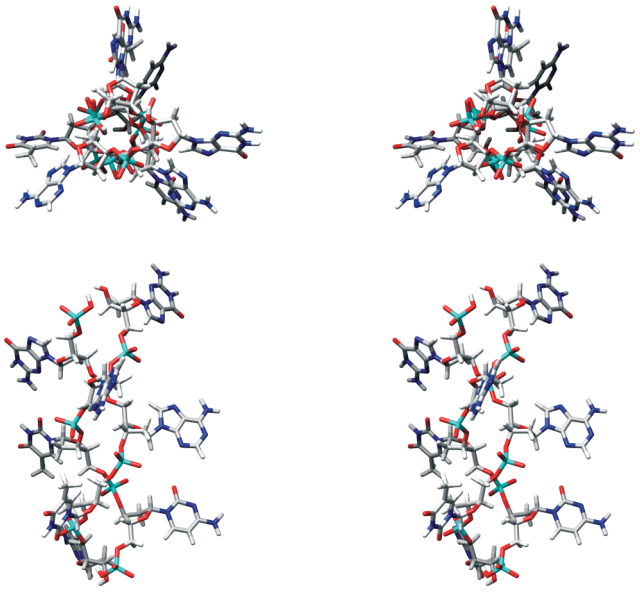

FIGURE 7: Stereo molecular model proposed for a segment of *Pf1*-DNA consisting of four arbitrary nucleotides of one strand [d(CpTpApG)] and four arbitrary nucleotides of the apposing antiparallel strand [d(GpApTpC)]. The intertwined strands are viewed along (top) and perpendicular (bottom) to the virion axis.

Val431, Lys445, Lys545, Lys645, and Leu743, while constraining the coordinates of all other atoms (nucleotide and amino acid). This procedure eliminated all unacceptable contacts and resulted in a significant energy reduction (~3 × 10^3 kcal/virion). The coordinates of the energy-minimized structure (Pf1N8P8) are available from the authors upon request.

DISCUSSION

The present study establishes that the nucleotides of the single-stranded DNA loop packaged within the Pf1 virion adopt specific orientations with respect to the filament axis. This finding is contrary to the inference of a random Pf1 DNA structure, which was proposed on the basis of fiber X-ray diffraction studies (*34*). The DNA base orientations determined from the polarized Raman measurements and the sugar−phosphate conformations deduced by Day and co-workers (*1*) allow us to propose a novel structure for the packaged Pf1 DNA molecule in which each nucleotide interacts stoichiometrically with a capsid subunit. The proposed *Pf1*-DNA structure exhibits many similarities to the Pauling-like *P*-DNA structure previously proposed by Allemand et al. (*25*), including values for the base rise and rotation of 6.10 Å and 131.8°, respectively, that compare favorably with those (5.85 Å and 137°) of *P*-DNA. Importantly, in both *Pf1*-DNA and *P*-DNA the bases project outwardly from the antiparallel sugar−phosphate chains that wind around one another to form the spine of the double helix. Two important differences may be noted between *Pf1*-DNA and *P*-DNA. (i) Whereas *P*-DNA is generated *in vitro* by applying mechanical stress to *B*-DNA, the structure of *Pf1*-DNA is proposed as the *in vivo* conformation of the packaged Pf1 genome. (ii) Whereas the bases on apposing antiparallel strands of *P*-DNA are complementary to one another (a consequence of stretching *B*-DNA), those of *Pf1*-DNA are not (owing to the genomic sequence).

In the proposed *Pf1*-DNA structure the glycosyl bond torsion angle chi (X), which is defined by the dihedral angle of either the pyrimidine O4′−C1′−N1−C2 or purine O4′−C1′−N9−C4

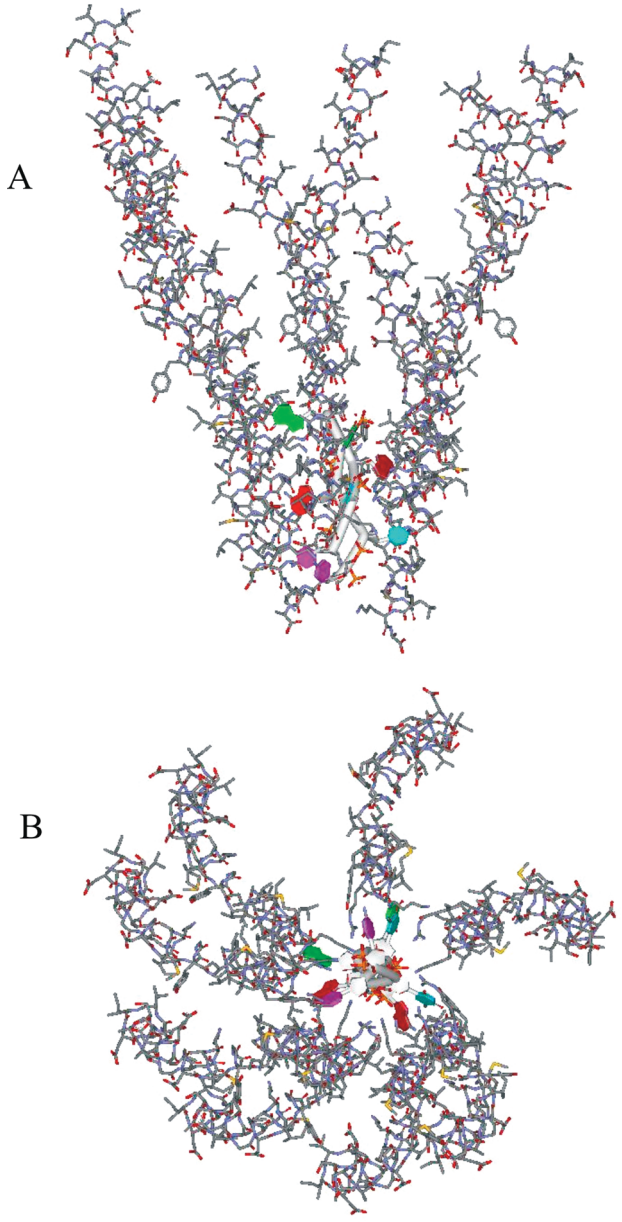

FIGURE 8: Molecular model proposed for the Pf1 viral assembly. The viral segment shown, which represents about $^{1}/_{1000}$th of the full virion length, consists of eight coat protein subunits and eight nucleotides of the packaged genome. Arbitrary sequences d(CpTpApG) and d(GpApTpC) are represented in the apposing DNA single strands. (A) View perpendicular to the virion axis. (B) View along the virion axis. Atomic coordinates of this model are available upon request from the authors.

nucleoside linkages, is −139° for dC, −137° for dT, −143° for dA, and −143° for dG. These are all within the so-called *anti* range (−90° > X > −270°). Thus, the X values of *Pf1*-DNA are similar to those of *B*-DNA, while distinct from those of *A*-DNA (*33*).

The base residues that project radially from the central axis of the packaged *Pf1*-DNA molecule make no apparent close contacts with neighboring capsid subunits (Figure 8). As previously suggested by Liu and Day (*1*), electrostatic interactions between basic side chains of the subunit C-terminus (Arg44 and Lys45) and DNA phosphates appear to be the basis of DNA/subunit interaction. Accordingly, virion assembly, which takes place within the periplasm of the host cell, presumably proceeds via extrusion of a covalently closed loop of single-stranded Pf1 DNA through the membrane in such a manner to allow nonspecific interaction between a nucleotide phosphate and subunit C-terminus in 1:1 stoichiometry.

ACKNOWLEDGMENT

The authors thank Dr. Loren Day (Public Health Research Institute) for providing access to unpublished data. We also thank Dr. Takumi Ueda (Graduate School of Pharmaceutical Sciences, University of Tokyo) for assistance with illustrations.

REFERENCES

1. Liu, D. J., and Day, L. A. (1994) Pf1 virus structure: helical coat protein and DNA with paraxial phosphates. *Science 265*, 671–674.
2. Overman, S. A., and Thomas, G. J., Jr. (2008) in Encyclopedia of Virology (Mahy, B. W. J., and van Regenmortel, M. H. V., Eds.) pp 190−198, Elsevier, Oxford, U.K.
3. Day, L. A., Marzec, C. J., Reisberg, S. A., and Casadevall, A. (1988) DNA packing in filamentous bacteriophages. *Annu. Rev. Biophys. Biophys. Chem. 17*, 509–539.
4. Welsh, L. C., Symmons, M. F., and Marvin, D. A. (2000) The molecular structure and structural transition of the alpha-helical capsid in filamentous bacteriophage Pf1. *Acta Crystallogr., Sect. D: Biol. Crystallogr. 56* (Part 2), 137–150.
5. Thiriot, D. S., Nevzorov, A. A., Zagyanskiy, L., Wu, C. H., and Opella, S. J. (2004) Structure of the coat protein in Pf1 bacteriophage determined by solid-state NMR spectroscopy. *J. Mol. Biol. 341*, 869–879.
6. Tsuboi, M., Kubo, Y., Ikeda, T., Overman, S. A., Osman, O., and Thomas, G. J., Jr. (2003) Protein and DNA residue orientations in the filamentous virus Pf1 determined by polarized Raman and polarized FTIR spectroscopy. *Biochemistry 42*, 940–950.
7. Zweckstetter, M., and Bax, A. (2001) Characterization of molecular alignment in aqueous suspensions of Pf1 bacteriophage. *J. Biomol. NMR 20*, 365–377.
8. Zweckstetter, M., and Bax, A. (2001) Single-step determination of protein substructures using dipolar couplings: aid to structural genomics. *J. Am. Chem. Soc. 123*, 9490–9491.
9. Thomas, G. J., Jr., Prescott, B., and Day, L. A. (1983) Structure similarity, difference and variability in the filamentous viruses fd, If1, IKe, Pf1, Xf and Pf3. *J. Mol. Biol. 165*, 321–356.
10. Cross, T. A., Tsang, P., and Opella, S. J. (1983) Comparison of protein and deoxyribonucleic acid backbone structures in fd and Pf1 bacteriophages. *Biochemistry 22*, 721–726.
11. Fritzsche, H., Tsang, P., Opella, S. J., and Kallenbach, N. R. (1986) Structure of the bacterial virus Pf1. An infrared linear dichroism study. *Stud. Biophys. 116*, 175–180.
12. Thomas, G. J., Jr., Prescott, B., Opella, S. J., and Day, L. A. (1988) Sugar pucker and phosphodiester conformations in viral genomes of filamentous bacteriophages: fd, If1, IKe, Pf1, Xf, and Pf3. *Biochemistry 27*, 4350–4357.
13. Nambudripad, R., Stark, W., and Makowski, L. (1991) Neutron diffraction studies of the structure of filamentous bacteriophage Pf1. Demonstration that the coat protein consists of a pair of alpha-helices with an intervening, non-helical surface loop. *J. Mol. Biol. 220*, 359–379.
14. Nambudripad, R., Stark, W., Opella, S. J., and Makowski, L. (1991) Membrane-mediated assembly of filamentous bacteriophage Pf1 coat protein. *Science 252*, 1305–1308.
15. Clack, B. A., and Gray, D. M. (1992) Flow linear dichroism spectra of four filamentous bacteriophages: DNA and coat protein contributions. *Biopolymers 32*, 795–810.
16. Kostrikis, L. G., Liu, D. J., and Day, L. A. (1994) Ultraviolet absorbance and circular dichroism of Pf1 virus: nucleotide/subunit ratio of unity, hyperchromic tyrosines and DNA bases, and high helicity in the subunits. *Biochemistry 33*, 1694–1703.
17. Wen, Z. Q., Armstrong, A., and Thomas, G. J., Jr. (1999) Demonstration by ultraviolet resonance Raman spectroscopy of differences in DNA organization and interactions in filamentous viruses Pf1 and fd. *Biochemistry 38*, 3148–3156.
18. Blanch, E. W., Bell, A. F., Hecht, L., Day, L. A., and Barron, L. D. (1999) Raman optical activity of filamentous bacteriophages: hydration of alpha-helices. *J. Mol. Biol. 290*, 1–7.
19. Tsuboi, M., Suzuki, M., Overman, S. A., and Thomas, G. J., Jr. (2000) Intensity of the polarized Raman band at 1340−1345 cm^{-1} as an

indicator of protein alpha-helix orientation: application to Pf1 filamentous virus. *Biochemistry 39*, 2677–2684.
20. Overman, S. A., Kristensen, D. M., Bondre, P., Hewitt, B., and Thomas, G. J., Jr. (2004) Effects of virion and salt concentrations on the Raman signatures of filamentous phages fd, Pf1, Pf3, and PH75. *Biochemistry 43*, 13129–13136.
21. Thiriot, D. S., Nevzorov, A. A., and Opella, S. J. (2005) Structural basis of the temperature transition of Pf1 bacteriophage. *Protein Sci. 14*, 1064–1070.
22. Marzec, C. J., and Day, L. A. (1983) DNA and protein lattice-lattice interactions in the filamentous bacteriophages. *Biophys. J. 42*, 171–180.
23. Day, L. A., Casadevall, A., Prescott, B., and Thomas, G. J., Jr. (1988) Raman spectroscopy of mercury(II) binding to two filamentous viruses: Ff (fd, M13, f1) and Pf1. *Biochemistry 27*, 706–711.
24. Wen, Z. Q., and Thomas, G. J., Jr. (1998) Ultraviolet resonance raman spectroscopy of DNA and protein constituents of viruses: assignments and cross sections for excitations at 257, 244, 238 and 229 nm. *Biopolymers 45*, 247–256.
25. Allemand, J. F., Bensimon, D., Lavery, R., and Croquette, V. (1998) Stretched and overwound DNA forms a Pauling-like structure with exposed bases. *Proc. Natl. Acad. Sci. U.S.A. 95*, 14152–14157.
26. Bustamante, C., Smith, S. B., Liphardt, J., and Smith, D. (2000) Single-molecule studies of DNA mechanics. *Curr. Opin. Struct. Biol. 10*, 279–285.
27. Wereszczynski, J., and Andricioaei, I. (2006) On structural transitions, thermodynamic equilibrium, and the phase diagram of DNA and RNA duplexes under torque and tension. *Proc. Natl. Acad. Sci. U.S.A. 103*, 16200–16205.
28. Tsuboi, M., and Thomas, G. J., Jr. (2007) in Protein Structures: Methods in Protein Structure and Stability Analysis (Uversky, V. N., and Permyakov, Eu. A., Eds.) pp 153−194, Nova Science Publishers, Hauppage, NY.
29. Tsuboi, M., and Thomas, G. J., Jr. (1997) Raman scattering tensors in biological molecules and their assemblies. *Appl. Spectrosc. Rev. 32*, 263–299.
30. Berkowitz, S. A., and Day, L. A. (1976) Mass, length, composition and structure of the filamentous bacterial virus fd. *J. Mol. Biol. 102*, 531–547.
31. Overman, S. A., Tsuboi, M., and Thomas, G. J., Jr. (1996) Subunit orientation in the filamentous virus Ff(fd, f1, M13). *J. Mol. Biol. 259*, 331–336.
32. Thomas, G. J., Jr., Benevides, J. M., Overman, S. A., Ueda, T., Ushizawa, K., Saitoh, M., and Tsuboi, M. (1995) Polarized Raman spectra of oriented fibers of A DNA and B DNA: anisotropic and isotropic local Raman tensors of base and backbone vibrations. *Biophys. J. 68*, 1073–1088.
33. Saenger, W. (1984) Principles of Nucleic Acid Structure, Springer-Verlag, New York.
34. Gonzalez, A., Nave, C., and Marvin, D. A. (1995) Pf1 filamentous bacteriophage: refinement of a molecular model by simulated annealing using 3.3 Å resolution X-ray fibre diffraction data. *Acta Crystallogr., Sect. D: Biol. Crystallogr. 51*, 792–804.
35. Brunger, A. T., Adams, P. D., Clore, G. M., Delano, W. L., Gross, P., Grosse-Kunstleve, R. W., Jiang, J.-S., Kuszewski, J., Nilges, M., Pannu, N. S., Read, R. J., Rice, L. M., Simonson, T., and Warren, G. L. (1998) Crystallography and NMR system. *Acta Crystallogr., Sect. D: Biol. Crystallogr. 54*, 905–921.
36. Overman, S. A., and Thomas, G. J., Jr. (1999) Raman markers of nonaromatic side chains in an alpha-helix assembly: Ala, Asp, Glu, Gly, Ile, Leu, Lys, Ser, and Val residues of phage fd subunits. *Biochemistry 38*, 4018–4027.